J Mater Sci (2017) 52:7539–7545

Nickel cobaltite@nanocarbon hybrid materials as efficient cathode catalyst for oxygen reduction in microbial fuel cells

Wei-Yan Xia[1,2], Liang Tan[1], Nan Li[1,*], Jie-Cheng Li[1], and Shao-Hao Lai[1]

[1] School of Chemistry and Chemical Engineering, Guangzhou University, Guangzhou 510006, China
[2] The Experimental School Affiliated to Guangzhou College, Guangzhou 510430, China

Received: 15 December 2016
Accepted: 8 March 2017
Published online: 16 March 2017

© Springer Science+Business Media New York 2017

ABSTRACT

The high efficiency of cathode catalyst used in the oxygen reduction reaction is a vital factor guaranteeing for the microbial fuel cells (MFCs). In this work, two novel nickel cobaltite@nanocarbon hybrids were rationally designed and successfully prepared as efficient cathode catalysts in air–cathode MFCs. Impressively, the achieved maximum power density of the MFCs equipped with $NiCo_2O_4$@MWCNTs cathode was about 356 mW m^{-2}, which is significantly higher than that of the MFCs with other cathodic catalysts. This work may provide not only the fundamental studies on nanocarbon-supported mixed-valent transition-metal oxides but also a new kind of promising alternative electrode in the technology of power generation from MFCs.

Introduction

The exploration of cost-effective non-noble metal electrocatalysts while maintaining the high performance of oxygen reduction reaction (ORR) catalysis is indispensable for future commercialization of the microbial fuel cells (MFCs) [1, 2]. MFCs, which utilize microorganisms as catalysts and harvest electricity from the oxidation of organic matter [3–5], possess distinct advantages compared with the conventional chemical fuel cells such as low operating temperature and environmental friendliness [6, 7]. Generally, platinum (Pt) as cathode catalyst is widely used to catalyze the ORR in the MFCs cathode, but hindered by its high cost and difficult acquirability [8]. Therefore, replacing the Pt-based cathode catalysts with inexpensive and high-efficient ORR catalysts is a significant pathway to the development of MFCs [9–11].

Up to now, other catalysts alternating with Pt-based materials including carbon materials [12] and inexpensive non-noble metal materials such as NiO [13], Co_3O_4 [14, 15], MnO_2 [16, 17], ZrO_2 [18] and Cu_2O [19] have been widely employed as ORR electrocatalysts for MFCs application. Moreover, carbon nanomaterials such as carbon nanotubes and graphene with unique electrical and structural properties have been extensively used as support material for the electrocatalysts to improve the electrical

Address correspondence to E-mail: nanli@gzhu.edu.cn

DOI 10.1007/s10853-017-0986-9

conductivity of electrode [20, 21]. However, it is still challenging to achieve satisfying ORR performance by means of inexpensive catalysts due to the sluggish kinetics of ORR. It was shown recently that mixed-valent transition-metal oxides were served as potential candidates for bifunctional catalysts in OER and ORR [22–24]. These results clearly outlined the potential of the mixed-valent transition-metal oxides for the development of high-performance and low-cost ORR catalyst.

In this work, we explored the feasibility of $NiCo_2O_4$ coated on the novel 3D hierarchical porous graphene-like (3D HPG) and multi-walled carbon nanotubes (MWCNTs) as cathode catalyst in single-chamber air–cathode MFCs owing to low cost but high performance. The catalysts were characterized by X-ray diffraction (XRD), transmission electron microscope (TEM) and electrochemical techniques, and its application was evaluated in the single-chamber air–cathode MFCs reactors. Particularly, the $NiCo_2O_4$@MWCNTs catalyst exhibited the best ORR performance and excellent stability, and it would further facilitate the scaling up of MFCs.

Experimental

Catalyst preparation

3D HPG was prepared according to the Li et al. [25] method. All other reagents were of analytical grade and were obtained from commercial sources. The MWCNTs and 3D HPG were treated in a 3:1 6 M H_2SO_4 and HNO_3 solution at 80 °C for 6 h before used.

$NiCo_2O_4$@3D HPG and $NiCo_2O_4$@MWCNTs were prepared through a typical heterogeneous reaction method. One millimole of Ni $(NO_3)_2{\cdot}6H_2O$, 2 mmol of $Co(NO_3)_2{\cdot}6H_2O$ and a certain of 3D HPG (or MWCNTs) were dissolved into deionized water (40 mL), followed by adding 5 mmol of NH_4F and 12 mmol of urea. After stirring for 1 h, the obtained homogeneous solution was transferred to Teflon-lined stainless steel autoclave and heated at 120 °C for 6 h. The resultant precipitate was washed several times with deionized water until the pH of the filtrate about 7 and dried in a vacuum oven overnight. Finally, the obtained powder was then annealed at 400 °C for 2 h in air. The pure $NiCo_2O_4$ catalyst was prepared by the same method without MWCNTs or 3D HPG.

Catalyst characterization

The crystal structure of materials was conducted by powder X-ray diffraction (Bruker, D8 ADVANCE) with Cu-Kα radiation. The morphology of the composite was observed with high-resolution transmission electron microscope (JEM-2010HR) at 200 kV. The structural properties of electrode materials were characterized by TEM (TEM, JEM-2010HR, 200 kV).

Electrode preparation and MFCs construction

Carbon cloths (not waterproofed, CeTech) were used as anodes. The various cathodes were prepared by coating corresponding catalyst on the waterproofed carbon cloth. The materials were mixed with 2% poly-tetrafluoroethylene suspension in ultrasonic bath, then brushed on the waterproofed carbon cloth with a loading of 4 mg cm^{-2} and dried at room temperature for 24 h.

The single-chamber air–cathode cuboid-shaped MFCs (volume 28 mL) were constructed and wired to an external resistance (1000 Ω). The cathode was located on one end of the MFCs with the hydrophobic side directly contacting with air and the catalyst-coated side facing the anode. The distance between the anode and cathode was fixed at 4 cm, and the efficient area of the electrodes was about 7 cm^2. Activated sludge from local city river (Guangzhou, China) was used as inoculums at the beginning. The culture medium consisted of glucose (1 g L^{-1}), trace elements (12.5 mL), vitamin solution (5 mL) and phosphate-buffered saline (PBS) nutrient medium which contained NH_4Cl (0.31 g L^{-1}), $NaH_2PO_4H_2O$ (1.3 g L^{-1}), $Na_2HPO_4{\cdot}3H_2O$ (9.4 g L^{-1}) and KCl (0.13 g L^{-1}) [26]. All MFCs tests were operated at 30 °C in constant temperature incubator, and the feeding solutions were refreshed when the voltage dropped below 0.05 V.

Measurement and analysis

All the voltages were recorded by data acquisition card (MPS010602, Beijing) for every minute. The power density curves and polarization curves were obtained by adjusting the external resistance values from 5000 to 40 Ω. All tests and analyses were carried out in two parallel samples. The power density P was calculated as $P = V \times I$. Both I and P were

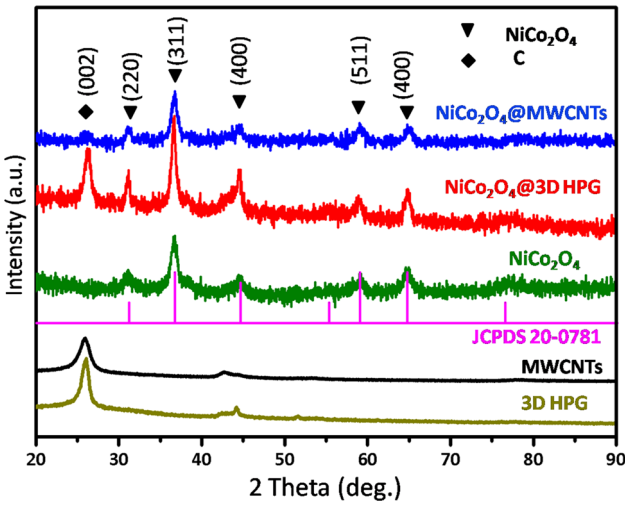

Figure 1 XRD patterns of 3D HPG, MWCNTs, $NiCo_2O_4$, $NiCo_2O_4$@3D HPG and $NiCo_2O_4$@MWCNTs.

normalized to the efficient area of cathode surface, and current density I was calculated using the formula of $I = V$ (cell voltage)$/(R \times A)$ (external resistance and efficient area).

Linear sweep voltammetry was applied to evaluate the electrochemical performance of the as-prepared catalysts. All of the electrochemical tests were carried out in 50 mM phosphate buffer solution (pH = 7) at room temperature with a CHI 760D workstation system (CH Instruments, Shanghai, China). An Ag/AgCl electrode was used as the reference electrode, and the Ag/AgCl electrode and Pt sheet (0.5 cm × 1 cm) were chosen as the reference and counter electrode, respectively. All the LSV tests were conducted at the oxygen-saturated surroundings, and the scan rate was 10 mV s^{-1} ranging from −0.5 to 0.5 V. In addition, electrochemical impedance spectroscopy (EIS) was performed in the frequency range of 100 kHz–0.01 Hz.

Results and discussion

Characterization of the $NiCo_2O_4$@3D HPG and $NiCo_2O_4$@MWCNTs composite

Typical XRD patterns of 3D HPG, MWCNTs, $NiCo_2O_4$, $NiCo_2O_4$@3D HPG and $NiCo_2O_4$@MWCNTs are shown in Fig. 1. Both 3D HPG and MWCNTs exhibited a basal reflection peak at $2\theta = 26.4°$, which corresponds to the (002) reflection of the graphitic planes. The strong diffraction peaks in all the patterns at the Bragg angles of 31.1°, 36.7°, 44.6°, 59.1° and 65.0° correspond to the (220), (311), (400), (511) and (440) diffraction peaks, which are similar to the XRD pattern of the $NiCo_2O_4$ (JCPDS

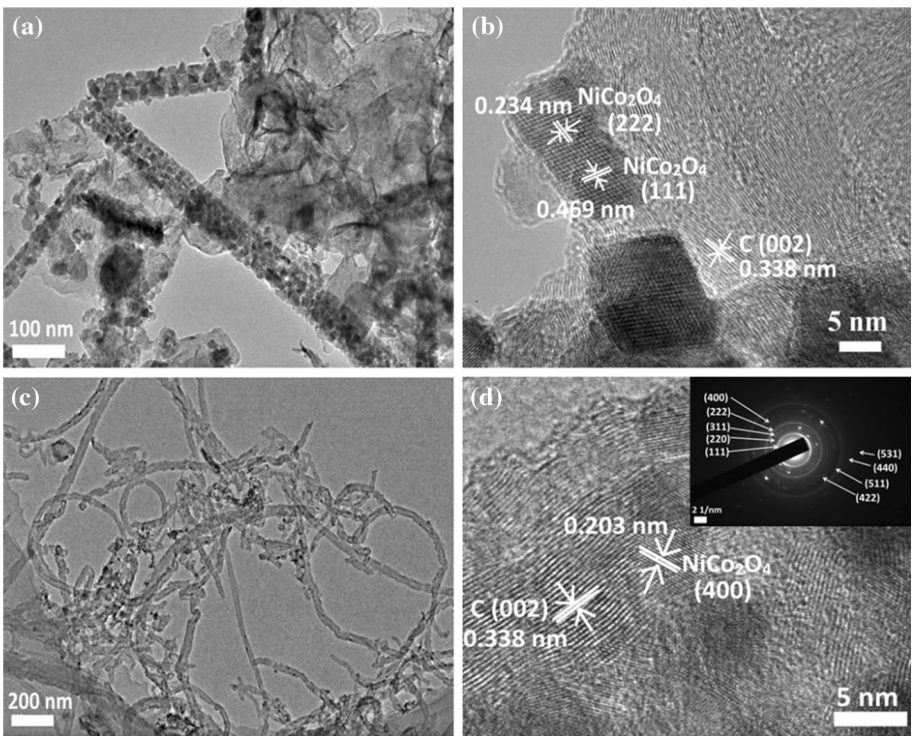

Figure 2 TEM images (**a** and **c**), HRTEM image (**b** and **d**) and SAED pattern (*inset* in **d**) of the $NiCo_2O_4$@3D HPG (**a** and **b**) and $NiCo_2O_4$@MWCNTs (**c** and **d**) composite.

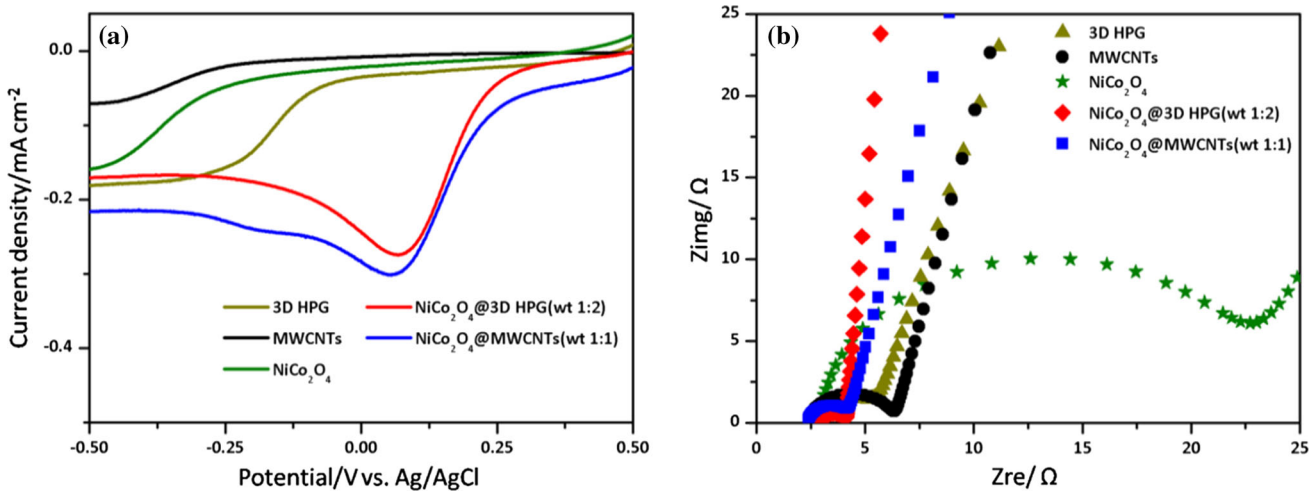

Figure 3 **a** LSV curves of different cathodes; **b** Nyquist plots of different electrodes measured by EIS technology with different electrodes.

20-0781). Moreover, the $NiCo_2O_4$@3D HPG and $NiCo_2O_4$@MWCNTs hybrids also clearly exhibited the characteristic peaks of $NiCo_2O_4$, indicating that the high purity of the as-prepared $NiCo_2O_4$@3D HPG and $NiCo_2O_4$@MWCNTs hybrids was obtained.

The morphology of the $NiCo_2O_4$@3D HPG and $NiCo_2O_4$@MWCNTs composites was examined by TEM which is presented in Fig. 2 at different magnifications. In Fig. 2a, c, there are a lot of $NiCo_2O_4$ nanoparticles distributed on the graphene and MWCNTs surface. From the high-resolution TEM (HRTEM) images (Fig. 2b, d), it's clear that many lattice fringes are coincided significantly with the planes of $NiCo_2O_4$. Furthermore, the selected-area electron diffraction (SAED) pattern also revealed the typical $NiCo_2O_4$@MWCNTs patterns that exhibiting single-crystalline hexagonal phase (inset in Fig. 2d). The observation from the above distinctly demonstrated that $NiCo_2O_4$@MWCNTs and $NiCo_2O_4$@3D HPG were obtained.

Electrochemistry performance

The ORR activity of catalysts was analyzed by linear sweep voltammetry. And all of the potential values were versus Ag/AgCl electrode. As shown in Fig. S3 and Fig. 3a, current–voltage curves without any significant peaks were obtained in the N_2-saturated electrolyte. Conversely, two obvious ORR peaks, in $NiCo_2O_4$@3D HPG (wt 1:2) and $NiCo_2O_4$@MWCNTs (wt 1:1) curves, can be observed when oxygen was introduced, indicating a electrochemical reduction in oxygen initiated on catalyst surface. The reduction peak of 0.081 V appeared at the $NiCo_2O_4$@3D HPG (wt 1:2), which was more positive than those at the $NiCo_2O_4$, 3D HPG and MWCNTs. However, $NiCo_2O_4$@MWCNTs (wt 1:1) shows a reduction peak at 0.056 V, which is a little more negative than $NiCo_2O_4$@3D HPG (wt 1:2). What's more, $NiCo_2O_4$@3D HPG (wt 1:2) and $NiCo_2O_4$@MWCNTs (wt 1:1) exhibited maximum current density (−0.272 and −0.302 mA cm^{-2}, respectively) at reduction peak. And the relative lower current density was recorded in the $NiCo_2O_4$, 3D HPG and MWCNTs. As a result, the electrode with $NiCo_2O_4$@MWCNTs (wt 1:1) showed the relative positive shifts of the reduction peak and the highest peak current density. Moreover, there is not obvious reduction peak in the pure $NiCo_2O_4$, indicating the enhanced ORR capacity may attribute to the efficient synergism between $NiCo_2O_4$ and carbon species [27, 28]. This phenomenon confirmed that adding $NiCo_2O_4$ into MWCNTs has higher catalytic activity toward oxygen reduction.

To better understand the influence of the materials on the MFCs, EIS experiments are conducted for different cathodes at open-circuit potential, and the Nyquist plots are shown in Fig. 3b. As the literature reported, the smaller the charge transfer resistance (R_{ct}), the faster the rate of charge transfer. The R_{ct} at electrode/electrolyte is equal to the diameter of the semicircle. The R_{ct} of $NiCo_2O_4$@3D HPG (wt 1:2) cathode was 1.13 Ω, which was less than those of pure $NiCo_2O_4$ (19.56 Ω) and 3D HPG (2.91 Ω), while the R_{ct} of $NiCo_2O_4$@MWCNTs (wt 1:1) cathode was

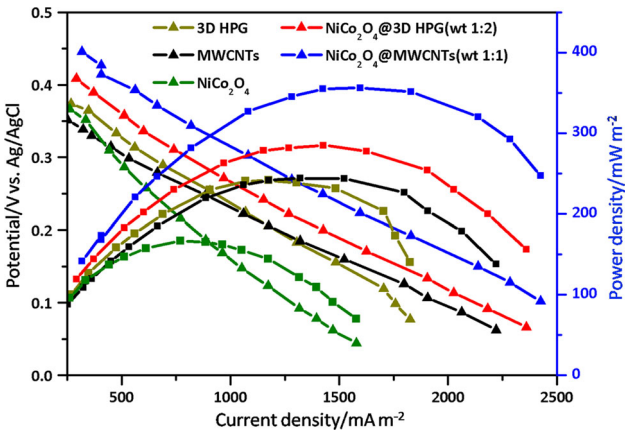

Figure 4 Power density as a function of current density and polarization curves for MFCs operated using different cathodes.

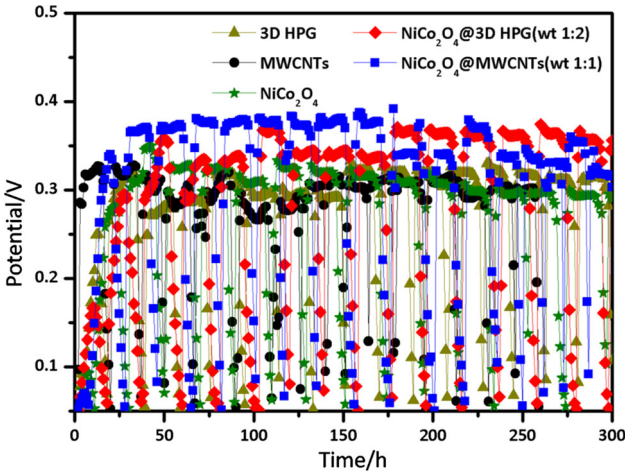

Figure 5 Representative cell voltage–time profile of MFCs equipped with different electrodes.

1.83 Ω, which was less than those of $NiCo_2O_4$ and MWCNTs (3.95 Ω). The observed lower R_{ct} of the prepared $NiCo_2O_4$@3D HPG and $NiCo_2O_4$@MWCNTs (wt 1:1) composite is resulted from the enhanced reaction rate kinetics and ascribed to the good micro/nanostructure for reactance to access the reaction centers.

MFCs performance

The $NiCo_2O_4$@3D HPG (wt 1:2) and $NiCo_2O_4$@MWCNTs (wt 1:1) were used as the cathode to assess the performance for power production in MFCs. For comparison, 3D HPG, MWCNTs and $NiCo_2O_4$ were used as controls. After the MFCs became stable, the MFCs performance was evaluated by plotting the polarization and power density curves. As shown in Fig. 4, the MFCs with $NiCo_2O_4$ cathode produced a maximum power density of only 166.49 mW m^{-2}, with the V_{oc} of 0.366 V. The MFCs with $NiCo_2O_4$@3D HPG catalysts produce satisfactory power output in terms of maximum power density (P_{max} = 285 mW m^{-2}) and open-circuit potential (V_{oc} = 0.408 V). At the same time, $NiCo_2O_4$@MWCNTs (wt 1:1) shows maximum power density (P_{max} = 356 mW m^{-2}) and open-circuit potential (V_{oc} = 0.446 V). Compared to the pure $NiCo_2O_4$, 3D HPG and MWCNTs, the combination of composites was avail to improve the power density and open-circuit voltage. As it turns out, $NiCo_2O_4$@MWCNTs (wt 1:1) with higher power density and circuit potential prove to be efficient and cost-effective cathode catalyst for practical MFCs applications.

In order to explore the best catalytic performance, different mass ratio of carbon materials and $NiCo_2O_4$ was investigated. In Figs. S1 and S2, the power density and polarization curves for the $NiCo_2O_4$@3D HPG and $NiCo_2O_4$@MWCNTs with different weight percent of $NiCo_2O_4$ were investigated. It can be seen that the power density increases with the increase in $NiCo_2O_4$ content but decreases again when it reaches a maximum value. The maximum power density of 285 and 356 mW m^{-2} was obtained from the $NiCo_2O_4$@3D HPG (wt 1:2) and $NiCo_2O_4$@MWCNTs (wt 1:1). This rule is the same with the open-circuit voltage of the composite with different mass ratio of $NiCo_2O_4$.

To further evaluate the durability of cathodic catalyst, cell voltages of different cathodes employed MFCs were examined as a function of time. The voltages produced in MFCs equipped with different cathodes are shown in Fig. 5. Reproducible cycles of electricity generation were obtained in all MFCs after inoculation. When the cell voltages of studied MFCs dropped to 0.05 V, the fresh inoculums were replaced. The voltages of MFCs rapidly increase upon the replacement of the fresh culture media, maintain its steady value for a period time and gradually decrease due to depletion of the substrate. Stable maximum voltages of 0.360 and 0.377 V are obtained for the MFCs with $NiCo_2O_4$@3D HPG (wt 1:2) and the MFCs with $NiCo_2O_4$@MWCNTs (wt 1:1). Among all the prepared catalysts, the $NiCo_2O_4$@MWCNTs (wt 1:1) composite exhibits excellent cycling behavior and durability.

Conclusion

A new type of carbon hybrid material consisted of $NiCo_2O_4$ nanoparticles grown on nanocarbon substrates was successfully obtained as cathode materials for MFCs. The as-prepared hybrids showed highly ORR catalytic activity and excellent stability in pH-neutral environment. The interesting results demonstrated that $NiCo_2O_4$/MWCNTs (wt% 1:1) materials could be a class of promising alternative cathode catalyst in ORR for MFCs applications.

Acknowledgements

This study was funded by Natural Science Foundations of Guangdong Province (Grant Number 2015A030313503) and Science and Technology Research Project of Guangzhou (Grant Number 201607010263).

Electronic supplementary material: The online version of this article (doi:10.1007/s10853-017-0986-9) contains supplementary material, which is available to authorized users.

References

[1] Xia W, Mahmood A, Liang ZB, Zou R, Guo S (2016) Earth-abundant nanomaterials for oxygen reduction. Angew Chem Int Ed 55:2650–2676

[2] Yuan H, Hou Y, Abu-Reesh IM, Chen J, He Z (2016) Oxygen reduction reaction catalysts used in microbial fuel cells for energy-efficient wastewater treatment: a review. Mater Horiz 3:382–401

[3] Ge Z, Li J, Xiao L, Tong Y, He Z (2014) Recovery of electrical energy in microbial fuel cells. Environ Sci Technol Lett 1:137–141

[4] Wang H, Park JD, Ren ZJ (2015) Practical energy harvesting for microbial fuel cells: a review. Environ Sci Technol 49:3267–3277

[5] Li WW, Yu HQ, He Z (2014) Towards sustainable wastewater treatment by using microbial fuel cells-centered technologies. Energy Environ Sci 7:911–924

[6] Rinaldi A, Mecheri B, Garavaglia V, Licoccia S, Nardo PD, Traversa E (2008) Engineering materials and biology to boost performance of microbial fuel cells: a critical review. Energy Environ Sci 1:417–429

[7] Sharma M, Bajracharya S, Gildemyn S, Patil SA, Alvarez-Gallego Y, Pant D, Rabaey K, Dominguez-Benetton X (2014) A critical revisit of the key parameters used to describe microbial electrochemical systems. Electrochim Acta 140:191–208

[8] Nie Y, Li L, Wei Z (2015) Recent advancements in pt and pt-free catalysts for oxygen reduction reaction. Chem Soc Rev 44:2168–2201

[9] Tang J, Liu J, Torad NL, Kimura T, Yamauchi Y (2014) Tailored design of functional nanoporous carbon materials toward fuel cell applications. Nano Today 9:305–323

[10] Zhou M, Wang HL, Guo S (2016) Towards high-efficiency nanoelectrocatalysts for oxygen reduction through engineering advanced carbon nanomaterials. Chem Soc Rev 45:1273–1307

[11] You S, Gong X, Wang W, Qi D, Wang X, Chen X, Ren N (2016) Enhanced cathodic oxygen reduction and power production of microbial fuel cell based on noble-metal-free electrocatalyst derived from metal-organic frameworks. Adv Energy Mater. doi:10.1002/aenm.201501497

[12] Daems N, Sheng X, Vankelecom IFJ, Pescarmona PP (2014) Metal-free doped carbon materials as electrocatalysts for the oxygen reduction reaction. J Mater Chem A 2:4085–4110

[13] Huang J, Zhu N, Yang T, Zhang T, Wu P, Zhi D (2015) Nickel oxide and carbon nanotube composite (NiO/CNT) as a novel cathode non-precious metal catalyst in microbial fuel cells. Biosens Bioelectron 72:332–339

[14] Gong XB, You SJ, Wang XH, Zhang JN, Gan Y, Ren NQ (2014) A novel stainless steel mesh/cobalt oxide hybrid electrode for efficient catalysis of oxygen reduction in a microbial fuel cell. Biosens Bioelectron 55:237–241

[15] Song TS, Wang DB, Wang H, Li X, Liang Y, Xie J (2015) Cobalt oxide/nanocarbon hybrid materials as alternative cathode catalyst for oxygen reduction in microbial fuel cell. Int J Hydrog Energy 40:3868–3874

[16] Liew KB, Wan RWD, Ghasemi M, Loh KS, Ismail M, Lim SS, Leong JX (2015) Manganese oxide/functionalised carbon nanotubes nanocomposite as catalyst for oxygen reduction reaction in microbial fuel cell. Int J Hydrog Energy 40:11625–11632

[17] Yuan H, Deng L, Qi Y, Kobayashi N, Hasatani M (2014) Morphology-dependent performance of nanostructured MnO_2 as an oxygen reduction catalyst in microbial fuel cells. Int J Electrochem Sci 10:3693–3706

[18] Mecheri B, Iannaci A, D'Epifanio A, Mauri A, Licoccia S (2016) Carbon-supported zirconium oxide as a cathode for microbial fuel cell applications. ChemPlusChem 81:80–85

[19] Zhang X, Li KX, Yan PY, Liu ZQ, Pu LT (2015) N-type Cu_2O doped activated carbon as catalyst for improving

power generation of air cathode microbial fuel cells. Bioresour Technol 187:299–304

[20] Tan L, Li N, Chen S, Liu ZQ (2016) Self-assembly synthesis of CuSe@graphene-carbon nanotubes as efficient and robust oxygen reduction electrocatalyst for microbial fuel cells. J Mater Chem A 4:12273–12280

[21] Lu M, Guo L, Kharkwal S, Wu H, Ng HY, Li SFY (2013) Manganese–polypyrrole–carbon nanotube, a new oxygen reduction catalyst for air-cathode microbial fuel cells. J Power Sources 221:381–386

[22] Ma TY, Zheng Y, Dai S, Jaroniec M, Qiao SZ (2014) Mesoporous $MnCo_2O_4$ with abundant oxygen vacancy defects as high-performance oxygen reduction catalysts. J Mater Chem A 2:8676–8682

[23] Liu ZQ, Cheng H, Li N, Ma TY, Su YZ (2016) $ZnCo_2O_4$ quantum dots anchored on nitrogen-doped carbon nanotubes as reversible oxygen reduction/evolution electrocatalysts. Adv Mater 28:3777–3784

[24] Cheng H, Su YZ, Kuang PY, Chen GF, Liu ZQ (2015) Hierarchical $NiCo_2O_4$ nanosheet-decorated carbon nanotubes towards highly efficient electrocatalyst for water oxidation. J Mater Chem A 3:19314–19321

[25] Li YY, Li ZS, Shen PK (2013) Simultaneous formation of ultrahigh surface area and three-dimensional hierarchical porous graphene-like networks for fast and highly stable supercapacitors. Adv Mater 25:2474–2480

[26] Tan L, Liu ZQ, Li N, Zhang JY, Zhang L, Chen S (2016) CuSe decorated carbon nanotubes as a high performance cathode catalyst for microbial fuel cells. Electrochim Acta 213:283–290

[27] Khilari S, Pandit S, Varanasi JL, Das D, Pradhan D (2015) Bifunctional manganese ferrite/polyaniline hybrid as electrode material for enhanced energy recovery in microbial fuel cell. ACS Appl Mater Interfaces 7:20657–20666

[28] Khilari S, Pandit S, Das D, Pradhan D (2014) Manganese cobaltite/polypyrrole nanocomposite-based air-cathode for sustainable power generation in the single-chambered microbial fuel cells. Biosens Bioelectron 54:534–540